The Plant Cell, Vol. 25: 1881–1894, May 2013, www.plantcell.org

Abnormal Glycosphingolipid Mannosylation Triggers Salicylic Acid–Mediated Responses in *Arabidopsis*[W][OA]

Jenny C. Mortimer,[a] Xiaolan Yu,[a] Sandra Albrecht,[a] Francesca Sicilia,[a,1] Mariela Huichalaf,[b] Diego Ampuero,[b,2] Louise V. Michaelson,[c] Alex M. Murphy,[d] Toshiro Matsunaga,[e,f] Samantha Kurz,[g] Elaine Stephens,[h,3] Timothy C. Baldwin,[i] Tadashi Ishii,[e] Johnathan A. Napier,[c] Andreas P.M. Weber,[g] Michael G. Handford,[b] and Paul Dupree[a,4]

[a] Department of Biochemistry, University of Cambridge, Cambridge CB2 1QW, United Kingdom
[b] Department of Biología, Facultad de Ciencias, Universidad de Chile, Las Palmeras 3425, Santiago, Chile
[c] Biological Chemistry Department, Rothamsted Research, Harpenden AL5 2JQ, United Kingdom
[d] Department of Plant Sciences, University of Cambridge, Cambridge CB2 3EA, United Kingdom
[e] Forestry and Forest Products Research Institute, Tsukuba, Ibaraki 305-8687, Japan
[f] National Agricultural Research Center, National Agriculture and Food Research Organization, Tsukuba, Ibaraki 305-8666, Japan
[g] Institute of Plant Biochemistry, Heinrich-Heine-Universität, 40225 Duesseldorf, Germany
[h] Department of Chemistry, University of Cambridge, Cambridge CB2 1EW, United Kingdom
[i] School of Applied Sciences, University of Wolverhampton, Wolverhampton WV1 1SB, United Kingdom

The *Arabidopsis thaliana* protein GOLGI-LOCALIZED NUCLEOTIDE SUGAR TRANSPORTER (GONST1) has been previously identified as a GDP-D-mannose transporter. It has been hypothesized that GONST1 provides precursors for the synthesis of cell wall polysaccharides, such as glucomannan. Here, we show that in vitro GONST1 can transport all four plant GDP-sugars. However, *gonst1* mutants have no reduction in glucomannan quantity and show no detectable alterations in other cell wall polysaccharides. By contrast, we show that a class of glycosylated sphingolipids (glycosylinositol phosphoceramides [GIPCs]) contains Man and that this mannosylation is affected in *gonst1*. GONST1 therefore is a Golgi GDP-sugar transporter that specifically supplies GDP-Man to the Golgi lumen for GIPC synthesis. *gonst1* plants have a dwarfed phenotype and a constitutive hypersensitive response with elevated salicylic acid levels. This suggests an unexpected role for GIPC sugar decorations in sphingolipid function and plant defense signaling. Additionally, we discuss these data in the context of substrate channeling within the Golgi.

INTRODUCTION

The plant Golgi apparatus provides an environment for the biosynthesis of noncellulosic cell wall polysaccharides and the glycosylation and sorting of lipids and proteins. The substrates for these processes are nucleotide sugars, the majority of which are UDP-linked, but GDP-D-Man (GDP-Man), GDP-D-Glc (GDP-Glc), GDP-L-Fuc (GDP-Fuc), and GDP-L-Gal (GDP-L-Gal) are also key (Bar-Peled and O'Neill, 2011). GDP-Man and GDP-Glc are substrates for glucomannan synthesis, GDP-Fuc is required for xyloglucan (XyG) and arabinogalactan fucosylation, and the pectin rhamnogalacturonan II (RG-II) is built from many nucleotide sugars including GDP-Fuc and GDP-L-Gal (Bar-Peled and O'Neill, 2011). GDP-Man is also a substrate for the endoplasmic reticulum–localized synthesis of protein *N*-linked glycan precursors and protein glycosylphosphatidyl inositol anchors, but no GDP-Man transporter is required since this sugar nucleotide is utilized at the cytosolic face of the membrane, either directly by mannosyltransferases or to generate dolichol-P-Man that is the direct precursor for endoplasmic reticulum luminal synthesis (Kinoshita et al., 2008; Jadid et al., 2011). GDP-Man is also an intermediate in L-ascorbic acid (AsA) biosynthesis in the cytosol (Wheeler et al., 1998; Conklin et al., 1999). A knockout *Arabidopsis thaliana* mutant in the GDP-Man pyrophosphorylase, *cytokinesis-defective1*, is embryo lethal (Nickle and Meinke, 1998; Lukowitz et al., 2001). A plant with a partially defective mutation in this gene, *vtc1*, has reduced AsA, *N*-glycosylation, and cell wall Man, making it difficult to interpret which of the many roles of GDP-Man cause the embryo phenotype (Conklin et al., 1997, 1999; Lukowitz et al., 2001). Moreover, there may be as yet unidentified roles for these nucleotide sugars, as many plant glycan structures are poorly characterized.

Most nucleotide sugars, and all GDP-sugars, are synthesized in the cytosol and therefore need to be translocated into the Golgi lumen to supply the luminal biosynthetic pathways. Fucosylation of XyG has been shown to require a GDP-Fuc transporter (Wulff et al., 2000). The CELLULOSE SYNTHASE LIKE A (CSLA) glucomannan synthases (Liepman et al., 2005; Goubet et al., 2009) have been proposed to have a luminal active site and therefore

[1] Current address: Sapienza Università di Roma, Rome 00185, Italy.
[2] Current address: Department of Biology, Institute of Pharmacy and Molecular Biotechnology, Heidelberg University, D-69120 Heidelberg, Germany.
[3] Current address: Blue Stream Laboratories, 763 Concord Ave., Cambridge, MA 02138.
[4] Address correspondence to p.dupree@bioc.cam.ac.uk.
The authors responsible for distribution of materials integral to the findings presented in this article in accordance with the policy described in the Instructions for Authors (www.plantcell.org) are: Jenny Mortimer (jm471@cantab.net) and Paul Dupree (p.dupree@bioc.cam.ac.uk).
[W] Online version contains Web-only data.
[OA] Open Access articles can be viewed online without a subscription.
www.plantcell.org/cgi/doi/10.1105/tpc.113.111500

require GDP-Man and GDP-Glc transport (Davis et al., 2010). Multiple nucleotide sugar transporter (NST) families have now been identified in *Arabidopsis* (Reyes and Orellana, 2008) and rice (*Oryza sativa*) (Seino et al., 2010; Zhang et al., 2011). Of those that have been functionally characterized to date, each has distinct substrate specificities (Baldwin et al., 2001; Norambuena et al., 2002; Handford et al., 2004, 2012; Bakker et al., 2005; Norambuena et al., 2005; Rollwitz et al., 2006). In *Arabidopsis*, we previously identified the GOLGI-LOCALIZED NUCLEOTIDE SUGAR TRANSPORTER (GONST) family of NSTs on the basis of homology to GDP-sugar transporters in other organisms (Baldwin et al., 2001; Handford et al., 2004). GONST1-4 are all Golgi-localized proteins that can functionally complement the yeast Golgi GDP-Man transporter mutant *vrg4-2* (Baldwin et al., 2001; Handford et al., 2004). Given the high sequence similarity of all known GDP-sugar transporters, these four NSTs may together be solely responsible for the transport of the four GDP-sugars required for luminal glycosylation processes into the Golgi in *Arabidopsis*. It has been hypothesized that nucleotide sugar selectivity and sub-Golgi compartment localization of Golgi NSTs may allow substrate channeling, regulating the flow of substrates to specific glycosyltransferases (GTs) and biosynthetic pathways (Seifert et al., 2002). Consequently, NSTs with relatively broad specificity might be important for a specific biosynthetic pathway because their activity is coupled spatially to the activity of one or a few GTs.

Sugars decorate glycosphingolipids. The basic sphingolipid building block is ceramide, which is formed from a long chain base (LCB) linked to a fatty acid by acylation. Glycosylinositol phosphoceramides (GIPCs), probably the predominant sphingolipid class in the plasma membrane (PM) of plant cells, are formed by the addition of an inositol phosphate to the ceramide (via headgroup exchange with the phospholipid phosphatidylinositol) followed by glycosylation of the inositol head group (Hannun and Obeid, 2008; Wang et al., 2008; Pata et al., 2010). These are both Golgi-localized processes. The inositol phosphoceramide (IPC) is variably decorated with a hexuronic acid, hexoses, pentoses, and amino sugars (Carter et al., 1958, 1969; Carter and Koob, 1969; Hsieh et al., 1978, 1981; Markham et al., 2006; Buré et al., 2011). In the few plant species characterized to date, it seems that there is a dominant glycan structure, although the composition of this is species specific (Carter et al., 1958, 1969; Hsieh et al., 1978; Markham et al., 2006). In *Arabidopsis*, the composition is reported to be glucuronic acid (GlcA), Glc, and Ara, although the structures are not fully described (Markham et al., 2006; Markham and Jaworski, 2007; Buré et al., 2011). The biosynthetic glycosylation steps and substrates are essentially uncharacterized. Recent studies in *Arabidopsis* have suggested a role for the LCB and ceramide moieties in various signaling processes, including programmed cell death (PCD) (Liang et al., 2003; Chen et al., 2008; Wang et al., 2008) and abscisic acid–dependent closure of stomata (Ng et al., 2001; Coursol et al., 2003; Michaelson et al., 2009). However, the importance of the GIPC sugar head group is unknown.

Here, we extended the characterization of GONST1 selectivity in vitro, showing that it can transport all plant GDP-sugars. We then isolated and characterized the *Arabidopsis* mutant *gonst1* and a mutant in its closely related homolog, *gonst2*. Unexpectedly, the cell walls of these mutants and the *gonst1 gonst2* double mutant were undistinguishable from the wild type, but the plants were severely dwarfed and developed spontaneous leaf lesions. Investigation of other Golgi-localized glycosylation processes led us to identify altered GIPC sugar headgroups in *gonst1*. Our data lead us to conclude that GONST1 is a GDP-sugar transporter that specifically transports GDP-Man into the Golgi for GIPC glycosylation. The characterization of this GIPC glycosylation mutant demonstrates that the loss of Man from GIPCs has an unexpectedly severe effect on plant growth and development.

RESULTS

GONST1 Can Transport the Four Plant GDP-Sugars

Previously, we showed that the *Arabidopsis* protein GONST1 complements a yeast Golgi GDP-Man transporter mutant, *vrg4-2* (Baldwin et al., 2001). When GONST1 was expressed in tobacco (*Nicotiana tabacum*; see Supplemental Figure 1 online), we confirmed that it stimulates the transport of GDP-Man. Transport of GDP-L-Gal and GDP-Fuc was also promoted by this NST, whereas transport of UDP-sugars was unaffected. A recent study using purified GONST1 in a liposome assay confirmed that GONST1 is a GMP-antiporter that can transport GDP-Man, as well as the plastid purine-sugar nucleotide ADP-Glc (Colleoni et al., 2010). Therefore, using the liposome assay, we tested the ability of GONST1 to transport all four plant Golgi GDP-sugars (GDP-Man, GDP-Glc, GDP-Fuc, and GDP-L-Gal; Figure 1; see Supplemental Figure 1 online). GONST1 transported all four with similar selectivity, but did not transport UDP-Glc or UDP-Gal. These results suggest that GONST1 is a purine sugar–specific transporter that is relatively nonselective in vitro for the sugar moiety.

gonst1 Has a Severe Developmental Phenotype

To determine the in vivo role for GONST1, three allelic homozygous T-DNA insertional mutants were isolated. *gonst1-1* (Wassilewskija [Ws] ecotype), *gonst1-2*, and *gonst1-3* (both Columbia-0 [Col-0] ecotype) were confirmed as transcriptional knockouts (see Supplemental Figure 2 online). All three mutants showed a dwarfed phenotype with poor seed set (Figures 2A and 2B; see Supplemental Figure 2 online). All had spontaneous hypersensitive lesions (SHLs) on their leaves that appeared at ~14 d growth even under sterile conditions (this was less severe in the Ws background line *gonst1-1*; Figures 2A and 2C), and all grew very poorly on soil. GONST1 has a closely related homolog, GONST2, which is likely to have similar GDP-sugar specificity (Handford et al., 2004). A *gonst2* T-DNA insertion mutant lacking detectable transcript (Ws ecotype) was also isolated (*gonst2-1*; see Supplemental Figure 2 online). This mutant had no obvious developmental phenotype, but the *gonst1-1 gonst2-1* double mutant phenotype was more severe than *gonst1-1* alone, suggesting some redundancy with regards to transport of GDP-sugars.

Cell Wall Polysaccharides, Protein Glycosylation, and Ascorbate Synthesis Are Not Defective in *gonst1*

Since GONST1 is a Golgi-localized GDP-sugar transporter, we hypothesized that the growth defects of *gonst1* were due to

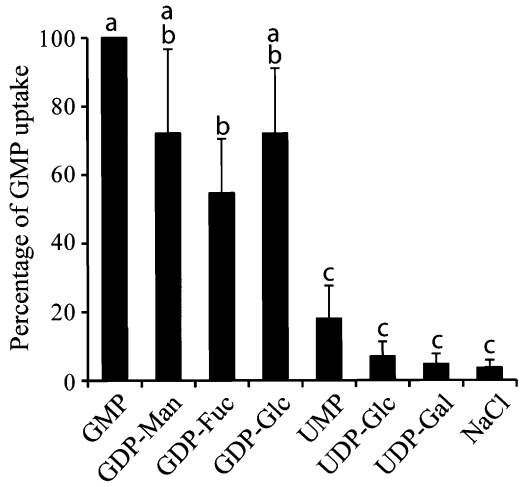

Figure 1. Substrate Specificity of GONST1.

GONST1 was expressed in yeast and the total membrane fraction isolated. Proteoliposomes were prepared and preloaded with 10 mM of the nucleotide sugar. The uptake was initiated by adding [^{14}C]-labeled GMP (corrected for background, calculated from yeast membranes lacking GONST1 expression). Data are presented compared with [^{14}C]GMP/GMP uptake, which was set to 100%. $n = 3 \pm$ SD. Letters indicate significant differences between genotypes (one-way analysis of variance and Tukey's honestly significant difference test, $P < 0.05$).

reduced availability of one or more of the four GDP-sugars required for polysaccharide biosynthesis. It has recently been proposed that CSLA9 uses luminal GDP-Man and GDP-Glc to synthesize glucomannan (Davis et al., 2010). Most Fuc in the cell wall arises from fucosylation of XyG, a process that requires a GDP-Fuc transporter (Wulff et al., 2000). To determine changes in cell wall composition, the noncellulosic monosaccharide composition of *gonst1* was analyzed by acid hydrolysis of alcohol-insoluble residue (AIR) prepared from callus and young plants (see Supplemental Table 1 online) and the stems of mature plants (Figure 2D). In all cases, the sugar composition of *gonst1* resembled the wild type. Moreover, this was true even for the severely dwarfed *gonst1 gonst2* double mutant (Figure 2D), indicating that the dwarfing was likely not due to changes in sugars in abundant polysaccharides.

Minor changes to polysaccharide structure may not be detectable in the total sugar composition analyses. In particular, glucomannan is a relatively low abundance polysaccharide in *Arabidopsis* (Handford et al., 2003). Immunofluorescent labeling with an antimannan antiserum revealed no difference between wild-type and *gonst1-1* mannan epitopes (Figure 2E). Calcofluor White staining showed normal stem morphology, albeit with a smaller stem diameter. Additionally, we analyzed glucomannan structure and quantity using polysaccharide analysis by carbohydrate gel electrophoresis (PACE; Figure 2F). No difference was observed between the wild-type and *gonst1* glucomannan PACE fingerprint. Together, these results clearly indicate that there is no detectable glucomannan deficiency in the *gonst1* mutants and that glucomannan deficiency is unlikely to cause the dwarfing phenotype.

Next, the structures of XyG and RG-II were investigated, since some components of both polysaccharides are synthesized from GDP-sugars. To determine if GONST1 is required for transport of GDP-Fuc for XyG biosynthesis, leaf AIR was hydrolyzed with xyloendoglucanase, and the resulting oligosaccharides analyzed by mass spectrometry (MS; Figure 3A). However, *gonst1-2* XyG structure was indistinguishable from the wild type, with normal levels of fucosylated side chains. In the *mur1-1* GDP-Fuc biosynthetic mutant, XyG fucosylation is substituted with L-Gal, since, in the absence of GDP-Fuc, the fucosyltransferase can use GDP-L-Gal (Zablackis et al., 1996; Reuhs et al., 2004). To investigate whether GONST1 is required for the transport of GDP-L-Gal for polysaccharide biosynthesis, we generated a *mur1-1 gonst1-2* double mutant. We hypothesized that this plant might be unable to replace the Fuc in the XyG and other polysaccharides with L-Gal, perhaps also resulting in a more severe growth phenotype. However, the growth of *mur1-1 gonst1-2* resembles *gonst1-2* (see Supplemental Figure 3A online). As previously reported, the *mur1-1* XyG lacked fucosylated structures (XXFG and XLFG) and contained substantial levels of L-galactosylated side chains (XXJG; Figure 3A). In the double mutant *mur1-1 gonst1-2*, the XyG structure is unchanged compared with *mur1-1* (Figure 3A), indicating that the supply of GDP-L-Gal to the Golgi lumen does not require GONST1. Finally, to determine any role for GONST1 in GDP-Fuc or GDP-L-Gal supply for RG-II synthesis, the dimerization of RG-II was measured, as *mur1-1* has a loss of dimerization (O'Neill et al., 2001). Again, *gonst1* showed no significant difference in RG-II dimerization from the wild type (Figure 3B). These data together suggest that GONST1 is not essential for the transport of any GDP-sugars for polysaccharide biosynthesis.

N-linked glycans of glycoproteins may be fucosylated in the Golgi from the donor GDP-Fuc (Lerouge et al., 1998). Wild-type, *gonst1-1*, and *mur1-1* leaf protein was tested for the presence of *N*-glycan fucosylation (see Supplemental Figure 3B online) or xylosylation (as a control; see Supplemental Figure 3C online) epitopes by immunoblotting. Again, *gonst1-1* resembled the wild type, whereas *mur1-1*, as expected, lacked all fucosylation, indicating that GONST1 is not required for the supply of GDP-Fuc transport for protein *N*-glycosylation.

Cytosolic GDP-Man is a precursor to the antioxidant AsA (Wheeler et al., 1998) and *Arabidopsis* plants with reduced AsA show leaf lesions (Pavet et al., 2005) similar to the phenotype of *gonst1*. Although AsA synthesis is not associated with the endomembrane system, disruption of the flow of GDP-Man into the Golgi might indirectly result in perturbed AsA biosynthesis, leading to hydrogen peroxide (H_2O_2) accumulation. To investigate this, we measured AsA levels in leaves of mutant and wild-type plants. However, *gonst1-1* and *gonst1-2* AsA levels were not significantly different to their respective background ecotypes (Figure 3C).

Arabidopsis GIPCs Contain Man Sugar Decorations That Are Decreased in *gonst1*

IPCs are thought to be glycosylated in the Golgi; however, the headgroup structure and biosynthesis is poorly characterized, partly due to difficulties in isolating them. Three recent MS studies

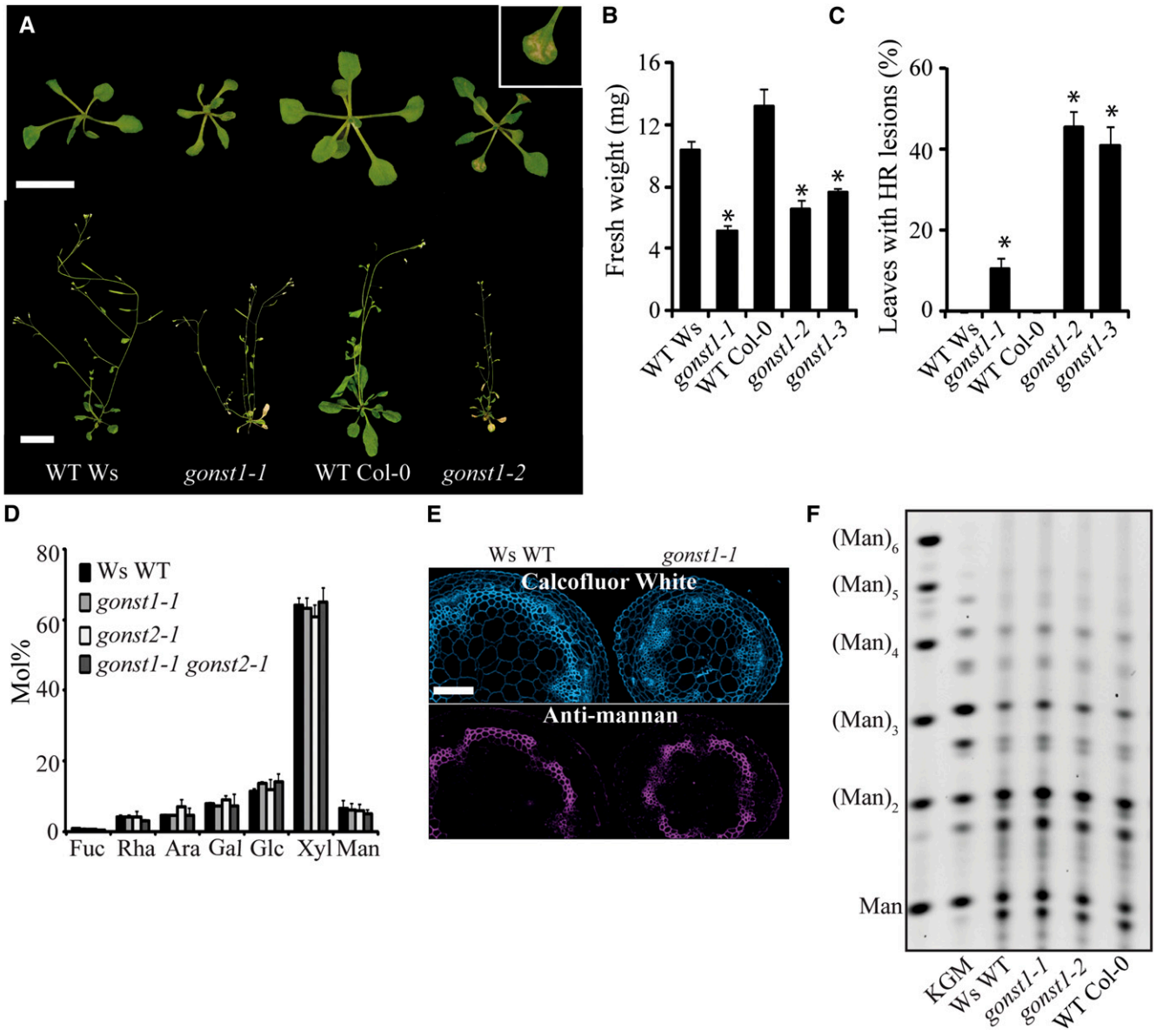

Figure 2. Phenotype of *gonst1*.

(A) Top row: 15-d-old, agar-grown wild type (WT) and *gonst1*. *gonst1-1* has a Ws background ecotype, whereas *gonst1-2* is Col-0. Bar = 1 cm. The inset shows a 15-d-old *gonst1-2* leaf, displaying spontaneous lesions. Bottom row: 5-week-old wild-type and *gonst1* soil-grown plants. Bar = 2.5 cm.
(B) and **(C)** Fresh weights of the rosettes **(B)** and percentage of leaves displaying hypersensitive lesions **(C)** of 15-d-old, agar-grown *gonst1-1*, *gonst1-2*, and *gonst1-3*, along with their respective wild types. $n = 21$ to 28 individual plants grown simultaneously; ±SE; asterisk indicates significant difference from the wild type (Student's t test, $P < 0.05$). HR, hypersensitive response.
(D) Neutral monosaccharide composition of aerial AIR from 6-week-old wild-type Ws, *gonst1-1*, *gonst2-1*, and *gonst1-1 gonst2-1* plants. AIR was hydrolyzed with 2 M TFA and analyzed by HPAEC-PAD. $n = 2$, ±SD.
(E) Immunofluorescent labeling of stem sections. Sections were labeled with an antibody specific to mannan, and cellulose was visualized with Calcofluor White. Bar = 100 μm.
(F) PACE fingerprint of mannan in stem cell wall. Oligosaccharides released from AIR by treatment with mannanases were derivatized with 8-aminonapthalene-1,3,6-trisulphonic acid and visualized by PACE. Konjac glucomannan (KGM) treated the same way is shown for comparison, along with $(Man)_{1-6}$ oligosaccharide standards. A representative gel from multiple experiments is shown.

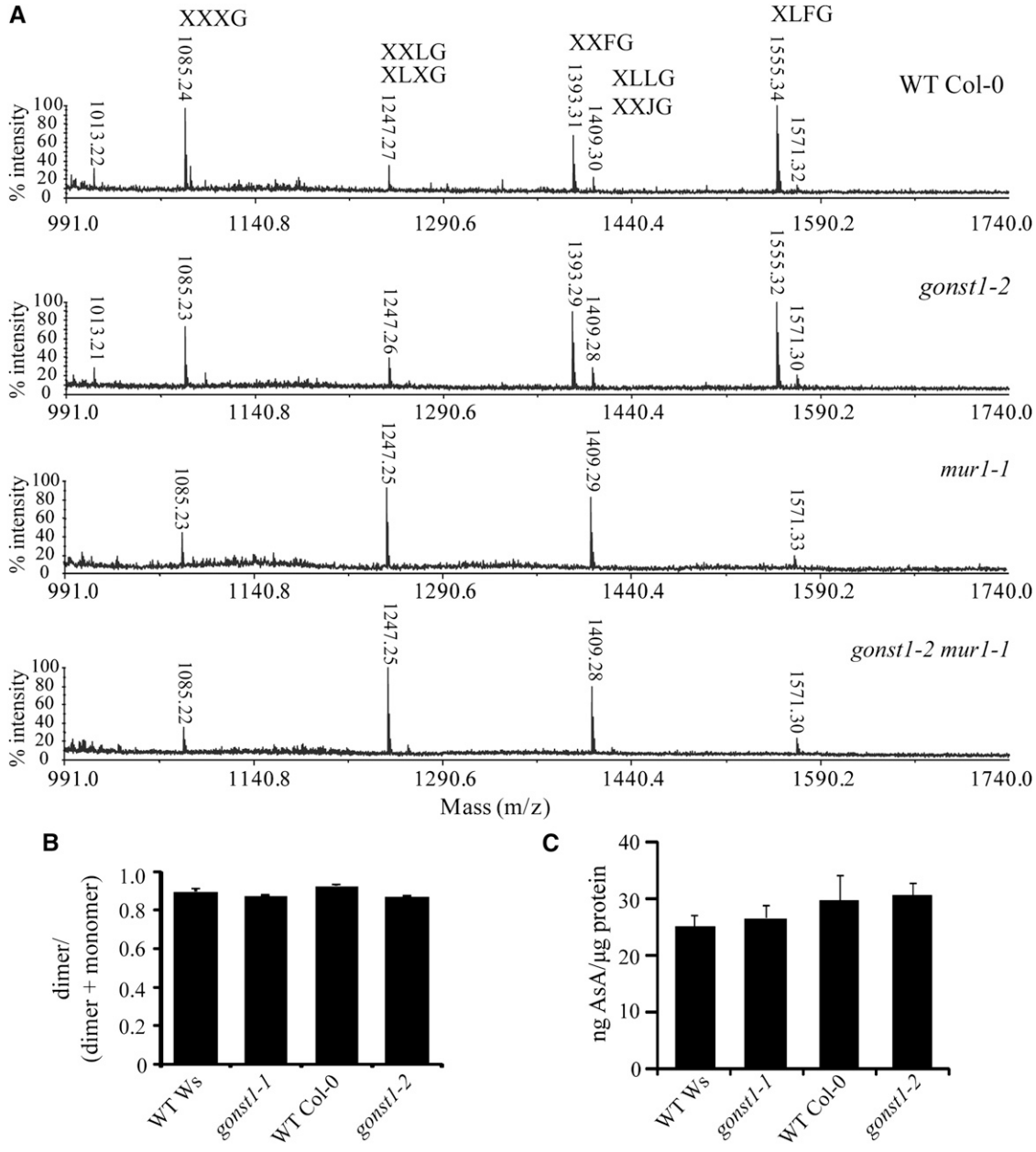

Figure 3. Further Characterization of *gonst1*.

(A) XyG structure. Leaf AIR was digested with xyloendoglucanase, and the resulting oligosaccharides analyzed by matrix-assisted laser desorption/ionization time of flight mass spectrometry. XyG structure of *gonst1-2* appears like wild-type (WT) Col-0, whereas *gonst1-2 mur1-1* resembles the Fuc biosynthetic mutant *mur1-1*, in which the oligosaccharides with Fuc mass 1393 (mass-to-charge ratio [*m/z*]) and 1555 (*m/z*) $[M+Na]^+$ are absent. Instead, the oligo with L-Gal (XXJG) of 1409.30 (*m/z*) $[M+Na]^+$ is increased.

(B) RG-II dimerization. AIR was digested with endopolygalacturonase, soluble material separated by size exclusion chromatography, and the ratio of RGII dimerization was measured by refractive index. $n = 2$, ±SD.

(C) AsA content of leaves; $n = 3$, +SD. For **(B)** and **(C)**, no significant difference was seen between the mutants and their respective wild type (Student's *t* test, $P < 0.05$).

have made progress on glycan headgroup analysis and reported the major *Arabidopsis* GIPC species as hexose-hexuronic acid-inositol phosphoceramide, where the Hex is considered to be a Glc and the hexuronic acid a GlcA residue (Markham et al., 2006; Markham and Jaworski, 2007; Buré et al., 2011). Here, we developed a method to isolate an enriched GIPC fraction from *Arabidopsis* callus total membranes, in order to simplify structural and compositional characterization. Ws, *gonst1-1*, Col-0, and *gonst1-2* GIPCs were then analyzed by liquid chromatography–tandem MS (LC-MS/MS) in multiple reaction monitoring (MRM)

mode according to Markham and Jaworski (2007) (see Supplemental Data Set 1 online), with increased numbers of transitions monitored to investigate possible additional GIPC species. The relative amounts of GIPCs containing none, one, or two hexose residues associated with HexA-Ins-P-Cer are shown in Figure 4A and Supplemental Data Set 1 online. Whereas *Arabidopsis* wild-type membranes contain mainly mono-hexosylated (Hex_1) GIPCs (~90%, depending on ecotype) and a minor proportion of dihexosylated GIPCs (Hex_2; ~10%), the proportion of Hex_1 GIPCs in membranes extracted from *gonst1* was drastically decreased to ~25%, and there was no evidence for Hex_2 species. Moreover, the majority (~75%) of *gonst1* GIPCs found were not hexosylated (Hex_0) and comprise only HexA in their headgroup. To determine which hexose was altered in the GIPCs, the monosaccharide composition of isolated GIPCs from wild-type and *gonst1* lines was analyzed. GlcA was detected, consistent with the published structures of GIPCs. Surprisingly, Ara, Gal, and Man were relatively abundant, in addition to the expected Glc. Interestingly, the only sugar with a significant decrease in *gonst1* was the hexose Man (Figure 4B), indicating that the defect in *gonst-1* is mannosylation of GIPCs.

To test whether the altered glycosylation of *gonst1* GIPCs affected other aspects of sphingolipid metabolism, a sphingolipidomic analysis of callus crude extract was performed according to Markham and Jaworski (2007), but again with increased numbers of GIPC transitions to monitor the GIPCs with altered headgroups (see Supplemental Figure 4 and Supplemental Data Set 1 online, with a summary shown in Figure 4C). The overall composition of ceramides, hydroxyceramides, glucosylceramides, GIPCs, and free LCBs in *gonst1* was similar compared with the wild type, indicating that the major change in GIPCs in the mutant is in the headgroups rather than the lipid moieties.

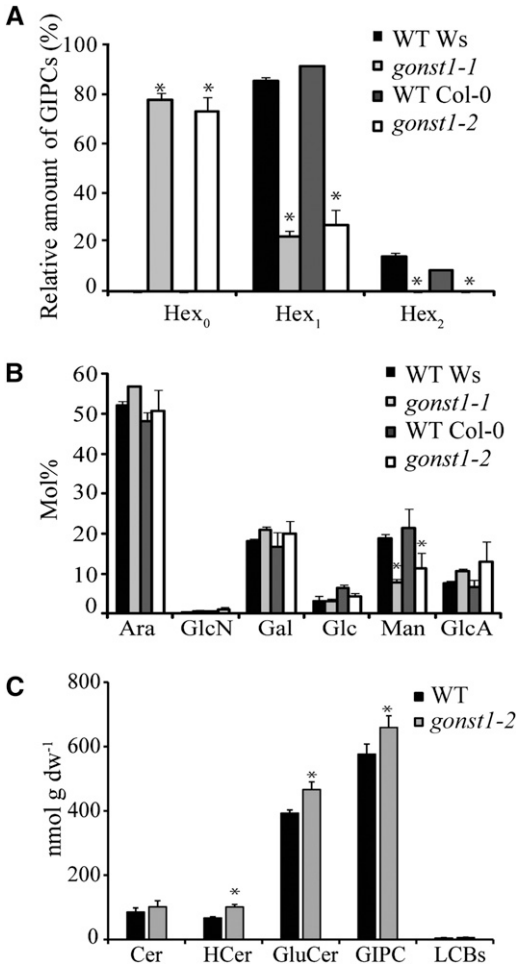

Figure 4. GIPC and Sphingolipidomic Analysis of the Wild Type and *gonst1*.

(A) GIPC headgroup hexose composition. GIPCs were isolated from the wild type (WT) and *gonst1* callus total membrane preparations. The GIPCs were analyzed by MS and categorized according to the number of hexoses in the sugar moiety (Hex_n). MRM was performed on a triple-quad mass spectrometer (QqQ-MS) for expected *m/z* (see Supplemental Data Set 1 online for details). Relative quantities were determined based on the peak areas of detected GIPCs, $n = 3$, ± SD.

(B) Monosaccharide composition of the isolated GIPC headgroups. Sugars were hydrolyzed with 2 M TFA and analyzed by HPAEC-PAD. Fuc, Rha, Xyl, and GalA were undetectable in these samples. $n = 3$, ±SD.

(C) Summary of sphingolipidomic analysis from whole callus extracts, as performed according to the method of Markham and Jaworski (2007); $n = 3$, ±SD (for detailed information, see Supplemental Figure 4 and Supplemental Data Set 1 online). Asterisks mark values significantly different from the wild type (Student's *t* test; $P < 0.05$). dw, dry weight.

gonst1 Displays a Constitutive Hypersensitive Response

To investigate the consequence of the defective GIPC glycosylation, we performed microarray analysis of Col-0 and *gonst1-2* 14-d-old leaves using the Affymetrix ATH1 array. Applying a P value of 0.05 and a fold change of >0.5 and <2, 123 genes were differentially expressed (0.54%; see Supplemental Data Set 2 online). Of the upregulated genes, those associated with the stress response were the most overrepresented in the data set (see Supplemental Data Set 2 online), including glutathione *S*-transferases (Dixon and Edwards, 2010) and peroxidases (Torres, 2010). Genes induced by salicylic acid (SA) and H_2O_2 (e.g., *PATHOGENESIS RESPONSE1* [*PR1*], *PR5* [Robert-Seilaniantz et al., 2011], and *WRKY8* [Chen et al., 2010]) were upregulated, along with genes which have been previously shown to be responsive to pathogen attack, such as *WALL ASSOCIATED KINASE LIKE10* (Meier et al., 2010), *SENESCENCE ASSOCIATED GENE13* (Brodersen et al., 2005), and *CHLOROPHYLLYASE1* (Kariola et al., 2005).

The SHL phenotype seen in *gonst1* is named for its similarity to lesions characteristic of the hypersensitive response in the presence of pathogens and resembles that seen in a group of mutants called lesion mimic mutants (LMMs) (reviewed in Lorrain et al., 2003). H_2O_2 and other reactive oxygen species are well characterized components of stress signal transduction pathways, and an excess can cause cell death. To determine if such a hypersensitive response was activated in *gonst1*, as indicated by the microarray data, leaves were incubated with 3,3-diaminobenzidine (DAB) to measure in situ H_2O_2 production (Figure 5A). As seen by the deposition of brown precipitate, both *gonst1-1* and *gonst1-2* accumulate H_2O_2 to a high level compared with the wild type, consistent with a constitutively active biotic stress response.

SA synthesis is triggered early during the hypersensitive cell death response, and this in turn potentiates cell death and more H_2O_2 accumulation (Vlot et al., 2009). To test whether elevated SA was contributing to the SHL phenotype, we quantified free and total SA in leaves of wild-type and *gonst1-2* plants. *gonst1-2* had increased pools of free and total SA (Figures 5B and 5C). To ascertain whether elevated SA is the cause of the growth phenotype and the necrotic lesion development, as has been demonstrated for other LMMs (e.g., *lesions simulating disease* [*lsd*] and *acd11*) (Weymann et al., 1995; Brodersen et al., 2002), *gonst1-2* was crossed with plants compromised in their ability to accumulate SA (Figure 6A). *NahG* encodes salicylate hydroxylase from *Pseudomonas fluorescens*, which converts SA to catechol and reduces intracellular SA accumulation when expressed in planta (Delaney et al., 1994). *isochorismate1* (*ics1*), a SA biosynthetic gene, has a 10- to 20-fold reduction in SA compared with the wild type (Wildermuth et al., 2001). Both *gonst1-2 NahG* and *gonst1-2 ics1-1* showed reduced H_2O_2 accumulation (Figure 6B), reduced SA (Figure 6C), and fewer SHLs (Figure 6D) and were larger than *gonst1-2* at maturity, although still dwarfed compared with the wild type (Figures 6A, 6E, and 6F). Therefore, elevated SA in *gonst1* is responsible, at least in part, for the dwarfing and necrotic lesion phenotypes.

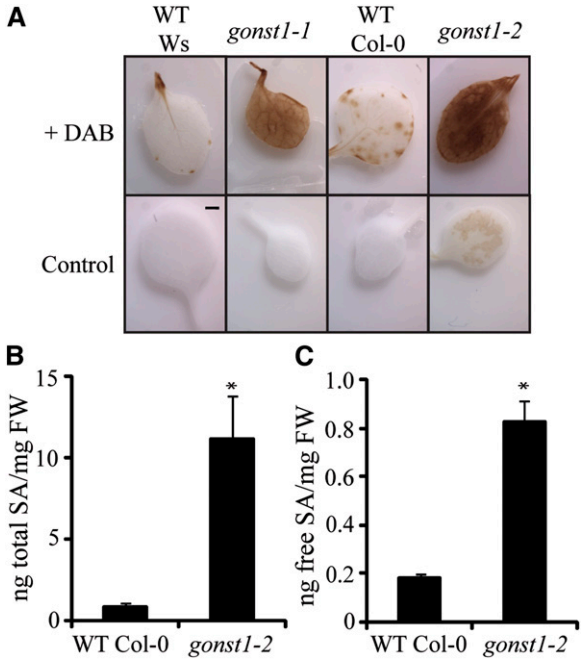

Figure 5. *gonst1* Exhibits a Constitutive Hypersensitive Response.

(A) Cellular H_2O_2 was detected using DAB. Leaves of 15-d-old, agar-grown plants were analyzed. Controls (leaves incubated without DAB) are shown alongside. Representative images are shown of three biological replicates. WT, the wild type.

(B) and **(C)** Total **(B)** and free **(C)** SA content of 15-d-old, agar-grown leaves. $n = 5$, $\pm$SD. Asterisks mark values significantly different from the wild type (Student's t test; $P < 0.05$). FW, fresh weight.

DISCUSSION

GIPCs, despite likely being the most abundant sphingolipid in the plant PM (Sperling et al., 2005), have historically been poorly characterized, both in terms of glycosidic decoration and function (Worrall et al., 2003; Sperling et al., 2005). In this study, we have shown that GONST1 can transport all four GDP-sugars in vitro; however, we present evidence that in planta, GONST1 is important specifically for the transport of GDP-Man into the Golgi for GIPC mannosylation. Phenotypic characterization of plants lacking GONST1 shows that, unexpectedly, these altered GIPC structures trigger the plant's defense response.

Previous work identified the four GONST NST family members as GDP-Man transporters, since all members can complement the yeast GDP-Man transporter *vrg4-2* (Baldwin et al., 2001; Handford et al., 2004). Consistent with this, in two different heterologous expression systems, GONST1 shows strong selectivity for GDP- over UDP-linked sugars. In vitro, GONST1 can transport all four plant GDP-sugars (GDP-Man, GDP-Glc, GDP-Fuc, and GDP-L-Gal), which is unexpected since previously characterized plant NSTs show specificity for a single NDP-sugar (with the exception of UTR1 and UTR7, both of which can transport UDP-Glc and UDP-D-Gal; Norambuena et al., 2002; Reyes et al., 2010; Handford et al., 2012).

In order to characterize the function of GONST1 in planta, we identified mutant plants, initially to test the hypothesis that GONST1 transports GDP-sugars for the synthesis of non-cellulosic cell wall polysaccharides, such as glucomannan (Baldwin et al., 2001; Handford et al., 2003; Davis et al., 2010). However, extensive characterization of *gonst1* revealed no defects in cell wall polysaccharides, despite the severely dwarfed phenotype. GONST2, a closely related homolog (Handford et al., 2004) is likely to transport GDP-sugars for a similar purpose, since *gonst1 gonst2* was more severely affected, suggesting some redundancy in function. GONST3 or GONST4 are therefore the most probable candidates for provision of GDP-Fuc and GDP-L-Gal sugars into the Golgi for cell wall polysaccharide synthesis, for example, for RG-II biosynthesis (Handford et al., 2004; Reyes and Orellana, 2008) and for fucosylation of XyG (Wulff et al., 2000). Glucomannan synthesis may also rely on GONST3 or GONST4 to supply Golgi luminal GDP-Man and GDP-Glc. Alternatively, the CSLA mannan synthases may obtain the substrate from the cytosol, as proposed for the CSLC glucan synthases and cellulose synthase (Davis et al., 2010).

The clear dwarfing and SHL phenotype of *gonst1* mutants led us to explore proposed roles for GDP-sugars in processes other than polysaccharide synthesis, including glycolipid biosynthesis. *Arabidopsis* glycosylated sphingolipids have historically been poorly characterized, but three recent articles have described substantial advances toward improving GIPC isolation and analysis, and as a result it has been proposed that *Arabidopsis* has one major species of GIPC: Glc-GlcA-IPC (Markham et al., 2006; Markham and Jaworski, 2007; Buré et al., 2011). In agreement with this, Hex-GlcA-IPC was the major species detected in *Arabidopsis* callus using our methods, although $(Hex)_2$-GlcA-IPC was also detected, as noted by Buré et al. (2011). However, previous studies assigned the Hex as Glc, although the evidence for this is not clear. *gonst1* lacked detectable $(Hex)_2$-GlcA-IPC species and had significantly less

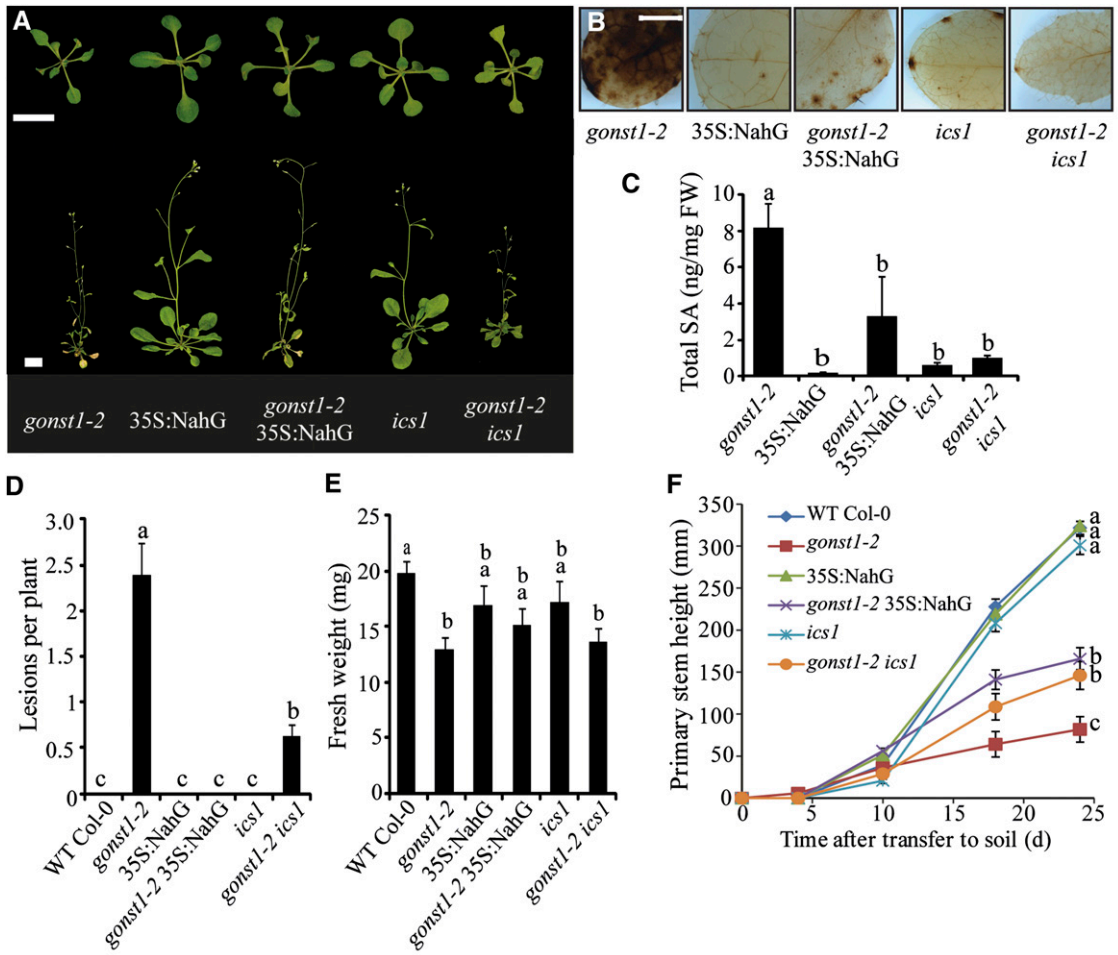

Figure 6. The *gonst1* Phenotype Can Be Partially Rescued by the Suppression of Salicylic Acid.

(A) *gonst1-2* was crossed with a plant expressing the bacterial salicylate hydroxylase gene (NahG) under the control of the cauliflower mosaic virus 35S promoter or with *ics1*, which has a lesion in an SA biosynthetic gene. Plants shown are as follows: top panel, 15 d old, agar grown, bar = 1 cm; bottom panel, 5 weeks old, soil grown, bar = 2.5 cm.

(B) Cellular H_2O_2 detected using DAB staining of 15-d-old, agar-grown leaves. Representative images of three biological replicates are shown. Bar = 1 mm.

(C) Total SA content of 15-d-old, agar-grown leaves (n = 3 to 5, ±SD). FW, fresh weight.

(D) and **(E)** Number of necrotic lesions per plant **(D)** and fresh weight of 15-d-old, agar-grown plants **(E)**. n = 10 to 23, ±SE. WT, the wild type.

(F) Stem height. Plants were transferred from agar to soil after 15 d of growth, and stem height was measured approximately every 7 d. Twelve plants per genotype were grown (two per cell), dispersed in a randomized pattern over three trays. Data shown are the mean ± SE. Letters indicate significant differences between genotypes (repeated-measures analysis of variance and Tukey's honestly significant difference test, $P < 0.05$).

Hex-GlcA-IPC compared with the wild type. Instead, more headgroups were detected that lacked any hexose. The monosaccharide composition of this GIPC fraction revealed that the only sugar that was significantly decreased in *gonst1* was Man, whereas Glc was unaffected. Therefore, we propose that the Hex on the major GIPC species detected in this study is Man. A sphingolipid-derived oligosaccharide with this composition was previously isolated from bean (*Phaseolus vulgaris*), rose (*Rosa* sp), and maize (*Zea mays*) (Carter et al., 1958, 1969; Carter and Koob, 1969; Smith and Fry, 1999), supporting our assignment. Our discovery that defective GDP-Man transport leads to defective GIPC synthesis has parallels with the phenotype of the yeast GDP-Man transporter mutant *vrg4*, which shows both a reduced growth rate (Poster and Dean, 1996) and a lack of mannosylated IPCs (Dean et al., 1997).

GONST1 transported all four GDP-sugars in vitro, and yet surprisingly the only altered glycosylation identified was a GIPC-specific Man deficiency, despite multiple uses for these substrates in the Golgi. Our studies imply the four closely related *Arabidopsis* GONST transporters may not be specific in the GDP-sugars they can transport, but nevertheless they provide substrates in vivo for different pathways. Indeed, GONST3 and GONST4 do not provide sufficient GDP-Man for the GIPC synthesis in our mutants, even though they can, in yeast studies

(Handford et al., 2003), transport GDP-Man. Therefore, these data support the substrate channeling hypothesis (Seifert et al., 2002), where GONST1 specifically provides GDP-Man for the as yet unidentified GIPC mannosyltransferase. This could be through a direct physical association between the NST and the GT or through localization of both proteins to a specific region of the Golgi stack.

The sugar composition of the *Arabidopsis* GIPC fraction from callus also revealed the presence of Gal and Ara residues. Ara and Gal residues have been reported on tobacco GIPCs (Hsieh et al., 1981; Sperling and Heinz, 2003), and a minor fraction of *Arabidopsis* GIPCs carrying multiple pentose residues were also recently identified from callus (although not leaves) (Buré et al., 2011). GIPCs containing pentoses weren't detected in our study, as the MRM transitions used in the sphingolipidomic profiling did not include these structures, but future work will aim to fully characterize these larger, more complex headgroups.

The *gonst1* phenotype can be classified as a severe member of the initiation subgroup of LMM, examples of which include some *acd* and *lsd* mutants (Lorrain et al., 2003). These mutants show activation of defense signaling in the absence of pathogens, SHL, and excess SA production. The correlative link between sphingolipid biosynthetic mutants and the SHL phenotype has been previously reported, for example, *acd11* (sphingosine transferase protein) (Brodersen et al., 2002), *acd5* (ceramide kinase) (Liang et al., 2003), and *loh1* (ceramide synthase) (Ternes et al., 2011), but not in connection with sphingolipid headgroups. Rather, it has been suggested that overaccumulation of ceramides acts as a signal for PCD (Wang et al., 2008), as has been reported in other systems (Poster and Dean, 1996; Hannun and Obeid, 2008). As discussed in a recent review (Markham et al., 2013), there is accumulating evidence that this link between elevated ceramide, SA, and PCD may not be direct but that other factors may be involved. For example, characterization of the fatty acid hydroxylation mutant *fah1 fah2* revealed elevated ceramides and SA, but the plant did not show a cell death phenotype under normal growth conditions (König et al., 2012). In support of this, *gonst1* does not have elevated ceramides, and unlike other sphingolipid mutants (e.g., *acd5*; Greenberg et al., 2000), the *gonst1* dwarfed phenotype is only partially rescued by crossing with NahG or *ics1* to suppress SA levels. Therefore, this suggests that the *gonst1* phenotype is not induced by alterations in lipid metabolism but is specifically due to GIPC headgroup alterations and that downstream effects on growth are acting via both a SA-mediated and SA-independent pathway.

gonst1 is a plant sphingolipid mutant that is altered in its GIPC glycosylation. It is now essential to work toward understanding why the loss of Man from the GIPC headgroup triggers SA and reactive oxygen species production. For instance, GIPCs may influence the structural properties of the PM or be involved in sorting or activation of the components of signal transduction networks within the PM, as has been described for sphingolipids in animal systems (Coskun et al., 2011). Indeed, GIPCs are known to be enriched in detergent resistant (lipid raft) fractions of the plant PM (Borner et al., 2005). Defects in cell surface components, such as arabinogalactan proteins (Gaspar et al., 2004) and callose (Nishimura et al., 2003), commonly result in a constitutively active defense responses, leading to the hypothesis that a mechanism exists by which the extracellular status of the cell can be reported (Nishimura et al., 2003). Since the GIPC headgroup is displayed on the cell surface, misglycosylation may be interpreted by this reporting system as evidence of pathogen attack. The difference between the phenotypic response of *gonst1* mutants in the Ws and Col-0 background may provide a tool to unpick the underlying genetics. Ws often shows less severe symptoms during pathogen infection than ecotype Col-0 (Kover and Schaal, 2002) because Ws is a naturally occurring mutant in the receptor kinase FLS2 (Chinchilla et al., 2006).

The improved GIPC analysis methods developed here and by others (Markham et al., 2006; Markham and Jaworski, 2007; Buré et al., 2011), combined with the understanding that a change to the glycosylation of these species has a major phenotypic effect, will encourage the rapid isolation and characterization of further plants with altered GIPC glycosylation. This should lead to insights into GIPC function and an understanding of the mechanistic link between GIPC misglycosylation and SA signaling.

METHODS

All water used was 18.2Ω quality (MilliQ). All images were processed using Adobe Photoshop and Illustrator.

Plant Material and Growth Conditions

Arabidopsis thaliana seeds were surface sterilized and sown on solid medium containing 0.5× Murashige and Skoog salts including vitamins and 1% Suc (w/v). Following stratification (48 h, 4°C, in the dark), plates were then transferred to a growth room (21°C, 100 μmol m^{-2} s^{-1}, 16 h light/8 h dark, 60% humidity). After 2 to 3 weeks, plants were transferred either to soil (Levington M3) or to Magenta boxes containing the same solid media, under the same growth conditions. Liquid callus cultures were derived from *Arabidopsis* roots and maintained as described previously (Prime et al., 2000). All experiments were performed on at least three independently grown biological replicates, unless otherwise stated.

Mutant Identification

Seeds of T-DNA mutants in At2g13650 (*gonst1-1*, FLAG_164D07; *gonst1-2*, SALK_043593; and *gonst1-3*, GABI-Kat 207E06), At1g07290 (*gonst2-1*, FLAG_406C01), and At3g51660 (*mur1-1*) were obtained from the Nottingham Arabidopsis Stock Centre (NASC), Nottingham, UK; GABI-Kat, Bielefeld, Germany; and Institut National de la Recherche Agronomique, Versailles, France. Plants homozygous for the T-DNA insertions were identified by PCR. In order to identify transcriptional knockouts, RNA was extracted using the RNeasy kit (Qiagen), and cDNA synthesis was performed according to the manufacturer's instructions. PCR conditions for all reactions were as follows: (1) 94°C for 2 min; (2) 10 cycles of 94°C for 15 s, 55°C for 30 s, and 68°C for 1 min; (3) 25 cycles of 94°C for 15 s, 55°C for 30 s, and 68°C for 1 min + 5 s per cycle; and (4) 68°C for 10 min. 35S:NahG (ecotype Col-0) was a kind gift from John Carr, and *ics1-1* (ecotype Col-0) was a kind gift from Alison Smith (both University of Cambridge, UK). *ics1-1* is a C→T point mutation and was detected by sequencing of the *ICS1* gene-gene PCR fragment. All primers pairs used are listed in Supplemental Table 2 online.

Radiolabeled Substrates

For the tobacco (*Nicotiana tabacum*) transport assays, the following substrates were used: UDP-D-[6-^{3}H]Glc (35 Ci/mmol; GE Healthcare),

GDP-L-[2-^{3}H]Fuc (16 Ci/mmol; Perkin-Elmer), and GDP-D-[U-^{14}C]Man (275 mCi/mmol; GE Healthcare). GDP-L-^{14}[C]Gal (47.1 pmol/μL with 10,175 cpm/μL) was synthesized and purified from GDP-D-[^{14}C]Man according to Major et al. (2005). The purity of the GDP-L-[^{14}C]Gal was verified by HPLC (Major et al., 2005) and PACE (Goubet et al., 2002).

For the liposome assays, the following substrates were used: GMP [α-^{32}P] (3000 Ci/mmol; Hartmann Analytic) and GDP-D-[U-^{14}C]Man (55 mCi/mmol; Hartmann Analytic). GDP-L-[^{14}C]Gal was synthesized as described above.

Yeast Growth and Liposome Uptake Assays

Expression of GONST1 was induced by diluting the yeast cultures to an OD_{600} of 0.5 in fresh synthetic medium containing 2% (w/v) Gal and 2% (w/v) Glc, respectively, as described previously (Linka et al., 2008). Yeast cells were collected by centrifugation after further incubation for 8 h at 30°C. Isolation of the yeast total membrane fraction, preloading of liposomes, and reconstitution of the recombinant protein were conducted as previously described (Linka et al., 2008). Transport assays were started by adding the [^{14}C]-nucleotide sugar or [^{14}C]-GMP, respectively. Transport reactions were stopped by loading aliquots of the proteoliposomes after defined time intervals (2, 4, 8, 16, 32, and 64 min) onto custom-made columns packed with anion exchange resin (Resin AG1-X8; Bio-Rad) that was preequilibrated with 150 mM sodium acetate buffer. Eluted proteoliposomes were collected, and the imported radiolabeled nucleotide sugar or GMP, respectively, was counted by liquid scintillation counting. Initial velocity of the transport reactions was determined by nonlinear regression using GraphPad Prism software (GraphPad Software). Since GDP-L-Gal is not commercially available, transport of custom-made [^{14}C]-GDP-L-Gal was followed into liposomes that were preloaded with 10 mM GMP.

Tobacco Leaf Transformation, Subcellular Fractionation, and Nucleotide-Sugar Uptake Assays

Tobacco leaves were used for *Agrobacterium tumefaciens*–mediated transformation (strain GV3101) with and without pVKH18-GONST1-GFP (Handford et al., 2004) by syringe infiltration (Norambuena et al., 2005). Five days after infiltration, transformed tobacco leaves were subcellularly fractionated (Ordenes et al., 2002), and Golgi-enriched fractions (50 μg protein) were incubated with the radiolabeled nucleotide-sugar (1 μM, 0.1 μCi) according to Norambuena et al. (2005).

AIR Preparation

Plant tissue (developmental stages as described in the results) was harvested, submerged in 96% (v/v) ethanol, and boiled at 70°C for 30 min to inactivate enzymes. Following homogenization using a ball mixer mill (Glen Creston), the pellet was collected by centrifugation (4000*g* for 15 min). The pellet was then washed with 100% (v/v) ethanol, twice with chloroform:methanol (2:1), followed by successive washes with 65% (v/v), 80% (v/v), and 100% (v/v) ethanol. The remaining pellet of AIR was air dried at 40°C overnight. Aqueous suspensions of AIR were prepared using a glass homogenizer.

Cell Wall Analysis

PACE was performed as follows: 500 μg AIR was incubated with concentrated NH_3 for 30 min at 21°C and then dried in vacuo. Samples were resuspended in 0.1 M ammonium acetate (500 μL, pH 6.0), incubated overnight with excess CjMan5A and CjMan26A, and digested to completion, along with 20 μg Konjac glucomannan (Sigma-Aldrich), as described by Goubet et al. (2009). Following derivatization with 8-aminonapthalene-1,3,6-trisulphonic acid (Invitrogen), samples were separated by PAGE, as previously described (Goubet et al., 2009). Gels were visualized with a G-box (Syngene), using long-wave UV tubes and a short-pass filter, and images captured using the GeneView software.

High Performance Anion Exchange Chromatography with Pulsed Amperometric Detection (HPAEC-PAD)

AIR (50 μg) was incubated in 2 M trifluoroacetic acid (TFA) for 1 h at 120°C and dried in vacuo. Following resuspension in 200 μL water, the released monosaccharides were analyzed on a Dionex ICS3000 ion chromatography system equipped with a PA20 analytical column, PA20 guard column, borate trap, and a pulsed amperometric detector. To separate neutral sugars, the column was equilibrated with 12 mM KOH prior to injection. Five minutes after injection, the eluant concentration was decreased to 1 mM for a further 20 min, and this was followed by a wash step (100 mM, 5 min). Post-column addition of 100 mM KOH was performed to increase the detector sensitivity. To separate acidic sugars, the column was equilibrated in 96% A (100 mM NaOH) and 4% B (500 mM NaAc and 100 mM NaOH). After injection, % B was increased to 40% over 10 min and maintained for a further 10 min. A standard mixture, containing 25 μM of either neutral sugars (L-Fuc, L-rhamnose, L-Ara, D-Gal, D-Glc, D-Xyl, and D-Man) or acidic sugars (D-galacturonic acid and D-glucuronic acid) was run alongside each set of samples to allow quantitation.

Immunofluorescence

Sections were prepared and blocked as described (Handford et al., 2003), followed by incubation overnight at 4°C with the antimannan antisera (Handford et al., 2003) diluted 1:100 in blocking buffer (0.5% [v/v] fetal calf serum and 10% [v/v] goat serum in PBS, pH 7.2). The secondary antibody, Cy3-conjugated goat anti-rabbit (Jackson ImmunoResearch Laboratories), was diluted 1:100 in the blocking buffer and incubated with the sections for 1 h. Sections were then stained with Calcofluor white (0.1 mg mL^{-1} in PBS buffer) for 5 min and viewed on an Olympus BX61 microscope. The same exposure time was used for all antibody-labeled sections.

XyG Structure

Leaf AIR (100 μg) was incubated with 1 M NaOH (20 μL) for 2 h, and the pH adjusted to 5.0 with 0.5 M HCl. Samples were incubated overnight at 37°C with 250 μL 0.1 M ammonium acetate, pH 5.0, and 2 μL XEG5 (Pauly et al., 1999) (Novozymes). Following incubation at 100°C for 15 min to stop the reaction and centrifugation (14,000*g*, 15 min), the supernatant was filtered through a 3K MWCO Nanosep (Pall). The samples were lyophilized and the resulting oligosaccharides analyzed by matrix-assisted laser desorption/ionization time of flight mass spectrometry.

Protein Glycosylation

Leaf tissue (100 μg) was ground to a powder under liquid N_2, was incubated in 200 μL SDS-PAGE loading buffer containing 1 mM DTT for 5 min at 95°C, and centrifuged (16,000*g*, 5 min) to remove debris. Samples were separated by SDS-PAGE and glycosylation detected by immunoblotting using antibodies raised against either α(1,3)-Fuc or β(1,2)-Xyl from plant *N*-linked glycans, a kind gift from Véronique Gomord, University of Rouen, France (Faye et al., 1993).

RG-II Dimerization

RG-II dimerization was measured according to Matsunaga and Ishii (2006). AIR (~5 mg) was saponified with 0.1 M NaOH (1 mL) for 4 h at 4°C, and the pH was adjusted to 5.0 with 75 μL of 10% (v/v) acetic acid. The samples were digested overnight at 35°C with 5 μL (2.5 units) of endopolygalacturonase

(Megazyme), soluble material (100 μL) separated by size exclusion chromatography, and the ratio of RGII dimerization was measured by refractive index.

AsA Assay

AsA content of leaves was measured according to Gautier et al. (2009) with some modifications. Frozen tissue (~100 μg) was homogenized, resuspended in 200 μL of 6% (v/v) trichloroacetic acid, and vortexed until thawed. Following incubation on ice for 15 min, the sample was centrifuged (16,000*g*, 4°C, 15 min). The pellet was retained for protein quantitation, and the supernatant (20 μL) was incubated in a microtiter plate (37°C, 20 min) with 20 μL 5 mM DTT (in 0.4 M PO_4 buffer, pH 7.4), before adding 10 μL of 0.5% (w/v) *N*-ethylmaleimide. After 1 min at 21°C, 80 μL of color reagent was added (solution A: 31% [w/v] orthophosphoric acid, 4.6% [v/v] trichloroacetic acid, and 0.6% [w/v] $FeCl_2$; solution B: 4% [w/v] 2,2-dipyridyl in 70% [v/v] ethanol ; A:B, 2.75:1) and incubated at 37°C for 40 min. AsA acid standards (0 to 50 nmol) were included to allow quantitation. The plate was scanned at 550 nm using a Fluostar Optima plate reader (BMG).

GIPC Purification and Analysis

Purification of total cell membranes was performed as described (Borner et al., 2003) with slight modification. Briefly, callus tissue was resuspended in homogenization buffer and homogenized using a polytron (Kinematica) at 4°C. The homogenate was centrifuged three times for 10 min at 1600*g* to remove cell debris prior to pelleting the membrane suspension onto a 1.8 M Suc cushion at 140,000*g* for 35 min. The harvested membrane fraction was diluted fivefold in cold buffer (150 mM NaCl, 5 mM EDTA, and 25 mM Tris-HCl, pH 7.5) and centrifuged at 100,000*g* for 1.5 h. The resulting membrane pellets were resuspended in cold TNE and homogenized in a 1-mL Dounce glass homogenizer. All membrane preparations were frozen in liquid N_2 and stored at −80°C. To extract GIPCs, total cell membranes were incubated in 5 mL buffer A ($CHCl_3$/C_2H_5OH/18 M NH_3/water [10:60:6:24 v/v/v/v]) overnight at 21°C. After centrifugation (1100*g*, 30 min), the supernatant was transferred to a weak AEX SPE cartridge (Strata X-AW; Phenomenex) that had been equilibrated with $CHCl_3$. The following series of wash steps were performed using one column volume (3 mL): $CHCl_3$, $CHCl_3$/CH_3OH (2:1, 1:1, and 1:2 v/v), and CH_3OH and the cartridge allowed to dry overnight. Bound GIPCs were eluted with buffer A, dried under a N_2 stream, and analyzed either by LC-MS/MS or HPAEC-PAD. Analysis of GIPCs by LC-MS/MS was performed as described (Markham and Jaworski, 2007). Briefly, the GIPCs were resuspended in 1 mL of tetrahydrofuran (THF)/methanol/water (2:1:2 v/v/v) and 0.1% formic acid and 50 μL was analyzed on a 4000 QTRAP LC-MS/MS system (ABSciex) after HPLC using an Agilent 1200 fitted with a 100-μL sample loop. Separation was achieved on a SUPELCOSIL ABZ+Plus column 150 × 3 mm, 5-μm particle size held at 40°C. The sample was eluted at 1 mL min^{-1} with a binary gradient system consisting of solvent A, THF/methanol/5 mM ammonium formate (3:2:5v/v/v), and 0.1% formic acid, and solvent B, THF/methanol/5 mM ammonium formate (7:2:1v/v/v), and 0.1% formic acid. The gradient started at 25% B rising to 60% B over 14 min. At the end of the gradient, the %B was increased to 100% over 2 min and held at 100% B for an additional 1 min to ensure complete elution of all compounds from the column. The probe was vertically positioned 11 mm from the orifice and charged with 5000 V. The temperature was held at 650°C, GS1 was set at 90 p.s.i., GS2 at 50 p.s.i., curtain gas at 20 p.s.i., and the interface heater was engaged. Declustering potential and collision energy were taken from Markham and Jaworski (2007) or were as shown in Supplemental Data Set 1 online. Data were collected with Analyst (ABSciex) software and integrated using the Intelliquant algorithm. Peaks for individual GIPCs were assigned based on their MRM transition. Peak areas were used to determine the relative ratio of each peak compared with overall areas found.

LCB and Sphingolipidomic Analysis

LCB and sphingolipidomic extraction and analysis from *Arabidopsis* callus were performed exactly as described (Markham and Jaworski, 2007).

Microarray Analysis

Wild type Col-0 and *gonst1-2* seeds were sown onto agar (three independently grown biological replicates, 20 seeds per plate, single genotype per plate) as described above. Following stratification for 48 h at 4°C, plates were transferred to constant light and grown vertically (in a random order). After 14 d of growth, shoot tissue was harvested and snap frozen in liquid N_2. RNA was isolated as described using TRIzol (Invitrogen) according to the manufacturer's protocols and treated with RQ1 RNase-free DNase (Promega) to remove contaminating DNA. Samples were further cleaned using RNeasy columns (Qiagen). RNA quality was assayed using a Bioanalyzer (Agilent), and samples were hybridized to the ATH1 chip (Affymetrix) by the NASC microarray service (Nottingham University, UK). Data are available for download at NASCarrays (http://affymetrix.Arabidopsis.info/; experiment ID 544). Analysis was performed using FlexArray (Blazejczyk et al., 2007) with GC Robust Multi-array Average Multi-array Average normalization and an Empirical Bayes (Wright and Simon) significance test. Genes with a P value < 0.05 and a twofold log change from the wild type were considered significant for this study.

Measurements of SA and H_2O_2

Accumulation of free and total SA in *Arabidopsis* leaf tissue was determined by HPLC using previously published methods (Surplus et al., 1998). H_2O_2 was detected by DAB staining according to Weigel and Glazebrook (2002) as follows: leaves from 15-d-old agar-grown plants were detached and submerged either in 1 mL buffer (100 mM HEPES-KOH, pH 6.8) or 1 mg mL^{-1} DAB (Sigma-Aldrich) in buffer. Following 4 min of vacuum infiltration, leaves were incubated overnight in the growth chamber under 24 h light. Leaves were cleared with 96% (v/v) ethanol (30 min, 70°C), mounted in water, and imaged under a low-power microscope.

Accession Numbers

Arabidopsis Genome Initiative numbers for genes discussed in this article are as follows: GONST1, At2g13650; GONST2, At1g07290; MUR1, At3g51160; and ICS1, At1g74710.

Supplemental Data

The following materials are available in the online version of this article.

Supplemental Figure 1. Substrate Specificity of GONST1.

Supplemental Figure 2. GONST1 and GONST2 T-DNA Insertional Mutants.

Supplemental Figure 3. Further Characterization of *gonst1* Glycosylation.

Supplemental Figure 4. Sphingolipidomic Analysis.

Supplemental Table 1. Monosaccharide Composition of AIR Prepared from Callus and Agar-Grown Seedlings.

Supplemental Table 2. PCR Conditions and Primers Used in This Study.

Supplemental Data Set 1. GIPC and Sphingolipidomic Analysis of Callus from the Wild Type and *gonst1*.

Supplemental Data Set 2. Microarray Analysis of Wild-Type and *gonst1* Seedlings.

ACKNOWLEDGMENTS

We thank Zhinong Zhang of the University of Cambridge for excellent technical help in making and growing the callus lines, the NASC Microarray Centre (Nottingham University, UK) for performing the microarray hybridizations, and Lisa Goers (University of Cambridge, UK) and Sebastián Febres (Universidad de Chile, Chile) for assistance in setting up the ascorbate and GDP-L-Gal assays, respectively. This work was supported by Biotechnology and Biological Sciences Research Council Grants BB/D010446/1 and BB/G016240/1, as well as funding from the European Community's Seventh Framework Programme (FP7/2007-2013) under Grant Agreement 211982 (RENEWALL) (to P.D.). The work was also supported by Fondecyt Grants 11060470 and 1100129 (to M.H.). A.P.M.W. appreciates funding by Deutsche Forschungsgemeinschaft Grant WE 2231/6-1. Rothamsted Research receives grant-aided support from the Biotechnology and Biological Sciences Research Council.

AUTHOR CONTRIBUTIONS

J.C.M. performed most of the work, supported by X.Y. S.A., L.V.M., and J.A.N. conducted the lipid analysis. F.S. expressed GONST1 in yeast. M.G.H. isolated *gonst1-1* and together with M.H. and D.A. synthesized GDP-L-Gal and directed transport studies in tobacco. A.P.M.W. directed GONST1 liposome assays. S.K. conducted GONST1 liposome assays. T.I. and T.M. performed the RG-II analysis. A.M.M. performed the SA analysis. T.C.B. assisted the immunofluorescence studies. E.S. assisted the glycan MS. J.C.M. and P.D. wrote the article.

Received March 13, 2013; revised April 22, 2013; accepted May 2, 2013; published May 21, 2013.

REFERENCES

Bakker, H., Routier, F., Oelmann, S., Jordi, W., Lommen, A., Gerardy-Schahn, R., and Bosch, D. (2005). Molecular cloning of two *Arabidopsis* UDP-galactose transporters by complementation of a deficient Chinese hamster ovary cell line. Glycobiology **15:** 193–201.

Baldwin, T.C., Handford, M.G., Yuseff, M.I., Orellana, A., and Dupree, P. (2001). Identification and characterization of GONST1, a golgi-localized GDP-mannose transporter in *Arabidopsis*. Plant Cell **13:** 2283–2295.

Bar-Peled, M., and O'Neill, M.A. (2011). Plant nucleotide sugar formation, interconversion, and salvage by sugar recycling. Annu. Rev. Plant Biol. **62:** 127–155.

Blazejczyk, M., Miron, M., and Nadon, R. (2007). FlexArray: A Statistical Data Analysis Software for Gene Expression Microarrays. (Montreal, Canada: Génome Québec).

Borner, G.H., Lilley, K.S., Stevens, T.J., and Dupree, P. (2003). Identification of glycosylphosphatidylinositol-anchored proteins in *Arabidopsis*. A proteomic and genomic analysis. Plant Physiol. **132:** 568–577.

Borner, G.H., Sherrier, D.J., Weimar, T., Michaelson, L.V., Hawkins, N.D., Macaskill, A., Napier, J.A., Beale, M.H., Lilley, K.S., and Dupree, P. (2005). Analysis of detergent-resistant membranes in *Arabidopsis*. Evidence for plasma membrane lipid rafts. Plant Physiol. **137:** 104–116.

Brodersen, P., Malinovsky, F.G., Hématy, K., Newman, M.-A., and Mundy, J. (2005). The role of salicylic acid in the induction of cell death in *Arabidopsis* acd11. Plant Physiol. **138:** 1037–1045.

Brodersen, P., Petersen, M., Pike, H.M., Olszak, B., Skov, S., Odum, N., Jørgensen, L.B., Brown, R.E., and Mundy, J. (2002). Knockout of *Arabidopsis accelerated-cell-death11* encoding a sphingosine transfer protein causes activation of programmed cell death and defense. Genes Dev. **16:** 490–502.

Buré, C., Cacas, J.L., Wang, F., Gaudin, K., Domergue, F., Mongrand, S., and Schmitter, J.M. (2011). Fast screening of highly glycosylated plant sphingolipids by tandem mass spectrometry. Rapid Commun. Mass Spectrom. **25:** 3131–3145.

Carter, H.E., Gigg, R.H., Law, J.H., Nakayama, T., and Weber, E. (1958). Biochemistry of the sphingolipides. XI. Structure of phytoglycolipide. J. Biol. Chem. **233:** 1309–1314.

Carter, H.E., and Koob, J.L. (1969). Sphingolipids in bean leaves (*Phaseolus vulgaris*). J. Lipid Res. **10:** 363–369.

Carter, H.E., Strobach, D.R., and Hawthorne, J.N. (1969). Biochemistry of the sphingolipids. 18. Complete structure of tetrasaccharide phytoglycolipid. Biochemistry **8:** 383–388.

Chen, L., Zhang, L., and Yu, D. (2010). Wounding-induced WRKY8 is involved in basal defense in *Arabidopsis*. Mol. Plant Microbe Interact. **23:** 558–565.

Chen, M., Markham, J.E., Dietrich, C.R., Jaworski, J.G., and Cahoon, E.B. (2008). Sphingolipid long-chain base hydroxylation is important for growth and regulation of sphingolipid content and composition in *Arabidopsis*. Plant Cell **20:** 1862–1878.

Chinchilla, D., Bauer, Z., Regenass, M., Boller, T., and Felix, G. (2006). The *Arabidopsis* receptor kinase FLS2 binds flg22 and determines the specificity of flagellin perception. Plant Cell **18:** 465–476.

Colleoni, C., Linka, M., Deschamps, P., Handford, M.G., Dupree, P., Weber, A.P., and Ball, S.G. (2010). Phylogenetic and biochemical evidence supports the recruitment of an ADP-glucose translocator for the export of photosynthate during plastid endosymbiosis. Mol. Biol. Evol. **27:** 2691–2701.

Conklin, P.L., Norris, S.R., Wheeler, G.L., Williams, E.H., Smirnoff, N., and Last, R.L. (1999). Genetic evidence for the role of GDP-mannose in plant ascorbic acid (vitamin C) biosynthesis. Proc. Natl. Acad. Sci. USA **96:** 4198–4203.

Conklin, P.L., Pallanca, J.E., Last, R.L., and Smirnoff, N. (1997). L-ascorbic acid metabolism in the ascorbate-deficient *Arabidopsis* mutant *vtc1.* Plant Physiol. **115:** 1277–1285.

Coskun, U., Grzybek, M., Drechsel, D., and Simons, K. (2011). Regulation of human EGF receptor by lipids. Proc. Natl. Acad. Sci. USA **108:** 9044–9048.

Coursol, S., Fan, L.M., Le Stunff, H., Spiegel, S., Gilroy, S., and Assmann, S.M. (2003). Sphingolipid signalling in *Arabidopsis* guard cells involves heterotrimeric G proteins. Nature **423:** 651–654.

Davis, J., Brandizzi, F., Liepman, A.H., and Keegstra, K. (2010). *Arabidopsis* mannan synthase CSLA9 and glucan synthase CSLC4 have opposite orientations in the Golgi membrane. Plant J. **64:** 1028–1037.

Dean, N., Zhang, Y.B., and Poster, J.B. (1997). The VRG4 gene is required for GDP-mannose transport into the lumen of the Golgi in the yeast, *Saccharomyces cerevisiae*. J. Biol. Chem. **272:** 31908–31914.

Delaney, T.P., Uknes, S., Vernooij, B., Friedrich, L., Weymann, K., Negrotto, D., Gaffney, T., Gut-Rella, M., Kessmann, H., Ward, E., and Ryals, J. (1994). A central role of salicylic acid in plant disease resistance. Science **266:** 1247–1250.

Dixon, D.P., and Edwards, R. (2010). Glutathione transferases. The Arabidopsis Book **8:** e0131, doi/10.1199/tab.0131.

Faye, L., Gomord, V., Fitchette-Lainé, A.C., and Chrispeels, M.J. (1993). Affinity purification of antibodies specific for Asn-linked glycans containing alpha 1—>3 fucose or beta 1—>2 xylose. Anal. Biochem. **209:** 104–108.

Gaspar, Y.M., Nam, J., Schultz, C.J., Lee, L.-Y., Gilson, P.R., Gelvin, S.B., and Bacic, A. (2004). Characterization of the *Arabidopsis* lysine-rich arabinogalactan-protein AtAGP17 mutant (*rat1*) that results in a decreased efficiency of agrobacterium transformation. Plant Physiol. **135:** 2162–2171.

Gautier, H., Massot, C., Stevens, R., Sérino, S., and Génard, M. (2009). Regulation of tomato fruit ascorbate content is more highly dependent on fruit irradiance than leaf irradiance. Ann. Bot. (Lond.) **103:** 495–504.

Goubet, F., Barton, C.J., Mortimer, J.C., Yu, X., Zhang, Z., Miles, G.P., Richens, J., Liepman, A.H., Seffen, K., and Dupree, P. (2009). Cell wall glucomannan in *Arabidopsis* is synthesised by CSLA glycosyltransferases, and influences the progression of embryogenesis. Plant J. **60:** 527–538.

Goubet, F., Jackson, P., Deery, M.J., and Dupree, P. (2002). Polysaccharide analysis using carbohydrate gel electrophoresis: A method to study plant cell wall polysaccharides and polysaccharide hydrolases. Anal. Biochem. **300:** 53–68.

Greenberg, J.T., Silverman, F.P., and Liang, H. (2000). Uncoupling salicylic acid-dependent cell death and defense-related responses from disease resistance in the *Arabidopsis* mutant *acd5*. Genetics **156:** 341–350.

Handford, M., Rodríguez-Furlán, C., Marchant, L., Segura, M., Gómez, D., Alvarez-Buylla, E., Xiong, G.-Y., Pauly, M., and Orellana, A. (2012). *Arabidopsis thaliana* AtUTr7 encodes a Golgi-localized UDP-glucose/UDP-galactose transporter that affects lateral root emergence. Mol. Plant **5:** 1263–1280.

Handford, M.G., Baldwin, T.C., Goubet, F., Prime, T.A., Miles, J., Yu, X.L., and Dupree, P. (2003). Localisation and characterisation of cell wall mannan polysaccharides in *Arabidopsis thaliana*. Planta **218:** 27–36.

Handford, M.G., Sicilia, F., Brandizzi, F., Chung, J.H., and Dupree, P. (2004). *Arabidopsis thaliana* expresses multiple Golgi-localised nucleotide-sugar transporters related to GONST1. Mol. Genet. Genomics **272:** 397–410.

Hannun, Y.A., and Obeid, L.M. (2008). Principles of bioactive lipid signalling: Lessons from sphingolipids. Nat. Rev. Mol. Cell Biol. **9:** 139–150.

Hsieh, T.C., Kaul, K., Laine, R.A., and Lester, R.L. (1978). Structure of a major glycophosphoceramide from tobacco leaves, PSL-I: 2-deoxy-2-acetamido-D-glucopyranosyl(alpha1 leads to 4)-D-glucuronopyranosyl(alpha1 leads to 2)myoinositol-1-O-phosphoceramide. Biochemistry **17:** 3575–3581.

Hsieh, T.C., Lester, R.L., and Laine, R.A. (1981). Glycophosphoceramides from plants. Purification and characterization of a novel tetrasaccharide derived from tobacco leaf glycolipids. J. Biol. Chem. **256:** 7747–7755.

Jadid, N., Mialoundama, A.S., Heintz, D., Ayoub, D., Erhardt, M., Mutterer, J., Meyer, D., Alioua, A., Van Dorsselaer, A., Rahier, A., Camara, B., and Bouvier, F. (2011). DOLICHOL PHOSPHATE MANNOSE SYNTHASE1 mediates the biogenesis of isoprenyl-linked glycans and influences development, stress response, and ammonium hypersensitivity in *Arabidopsis*. Plant Cell **23:** 1985–2005.

Kariola, T., Brader, G., Li, J., and Palva, E.T. (2005). Chlorophyllase 1, a damage control enzyme, affects the balance between defense pathways in plants. Plant Cell **17:** 282–294.

Kinoshita, T., Fujita, M., and Maeda, Y. (2008). Biosynthesis, remodelling and functions of mammalian GPI-anchored proteins: Recent progress. J. Biochem. **144:** 287–294.

König, S., Feussner, K., Schwarz, M., Kaever, A., Iven, T., Landesfeind, M., Ternes, P., Karlovsky, P., Lipka, V., and Feussner, I. (2012). *Arabidopsis* mutants of sphingolipid fatty acid α-hydroxylases accumulate ceramides and salicylates. New Phytol. **196:** 1086–1097.

Kover, P.X., and Schaal, B.A. (2002). Genetic variation for disease resistance and tolerance among *Arabidopsis thaliana* accessions. Proc. Natl. Acad. Sci. USA **99:** 11270–11274.

Lerouge, P., Cabanes-Macheteau, M., Rayon, C., Fischette-Lainé, A.C., Gomord, V., and Faye, L. (1998). *N*-glycoprotein biosynthesis in plants: Recent developments and future trends. Plant Mol. Biol. **38:** 31–48.

Liang, H., Yao, N., Song, J.T., Luo, S., Lu, H., and Greenberg, J.T. (2003). Ceramides modulate programmed cell death in plants. Genes Dev. **17:** 2636–2641.

Liepman, A.H., Wilkerson, C.G., and Keegstra, K. (2005). Expression of cellulose synthase-like (*Csl*) genes in insect cells reveals that *CslA* family members encode mannan synthases. Proc. Natl. Acad. Sci. USA **102:** 2221–2226.

Linka, N., Theodoulou, F.L., Haslam, R.P., Linka, M., Napier, J.A., Neuhaus, H.E., and Weber, A.P. (2008). Peroxisomal ATP import is essential for seedling development in *Arabidopsis thaliana*. Plant Cell **20:** 3241–3257.

Lorrain, S., Vailleau, F., Balagué, C., and Roby, D. (2003). Lesion mimic mutants: Keys for deciphering cell death and defense pathways in plants? Trends Plant Sci. **8:** 263–271.

Lukowitz, W., Nickle, T.C., Meinke, D.W., Last, R.L., Conklin, P.L., and Somerville, C.R. (2001). *Arabidopsis cyt1* mutants are deficient in a mannose-1-phosphate guanylyltransferase and point to a requirement of *N*-linked glycosylation for cellulose biosynthesis. Proc. Natl. Acad. Sci. USA **98:** 2262–2267.

Major, L.L., Wolucka, B.A., and Naismith, J.H. (2005). Structure and function of GDP-mannose-3′,5′-epimerase: An enzyme which performs three chemical reactions at the same active site. J. Am. Chem. Soc. **127:** 18309–18320.

Markham, J.E., and Jaworski, J.G. (2007). Rapid measurement of sphingolipids from *Arabidopsis thaliana* by reversed-phase high-performance liquid chromatography coupled to electrospray ionization tandem mass spectrometry. Rapid Commun. Mass Spectrom. **21:** 1304–1314.

Markham, J.E., Li, J., Cahoon, E.B., and Jaworski, J.G. (2006). Separation and identification of major plant sphingolipid classes from leaves. J. Biol. Chem. **281:** 22684–22694.

Markham, J.E., Lynch, D.V., Napier, J.A., Dunn, T.M., and Cahoon, E.B. (March 13, 2013). Plant sphingolipids: Function follows form. Curr. Opin. Plant Biol. http://dx.doi.org/10.1016/j.pbi.2013.02.009.

Matsunaga, T., and Ishii, T. (2006). Borate cross-linked/total rhamnogalacturonan II ratio in cell walls for the biochemical diagnosis of boron deficiency in hydroponically grown pumpkin. Anal. Sci. **22:** 1125–1127.

Meier, S., Ruzvidzo, O., Morse, M., Donaldson, L., Kwezi, L., and Gehring, C. (2010). The *Arabidopsis* wall associated kinase-like 10 gene encodes a functional guanylyl cyclase and is co-expressed with pathogen defense related genes. PLoS ONE **5:** e8904.

Michaelson, L.V., Zäuner, S., Markham, J.E., Haslam, R.P., Desikan, R., Mugford, S., Albrecht, S., Warnecke, D., Sperling, P., Heinz, E., and Napier, J.A. (2009). Functional characterization of a higher plant sphingolipid Δ4-desaturase: defining the role of sphingosine and sphingosine-1-phosphate in *Arabidopsis*. Plant Physiol. **149:** 487–498.

Ng, C.K., Carr, K., McAinsh, M.R., Powell, B., and Hetherington, A.M. (2001). Drought-induced guard cell signal transduction involves sphingosine-1-phosphate. Nature **410:** 596–599.

Nickle, T.C., and Meinke, D.W. (1998). A cytokinesis-defective mutant of *Arabidopsis* (*cyt1*) characterized by embryonic lethality, incomplete cell walls, and excessive callose accumulation. Plant J. **15:** 321–332.

Nishimura, M.T., Stein, M., Hou, B.-H., Vogel, J.P., Edwards, H., and Somerville, S.C. (2003). Loss of a callose synthase results in salicylic acid-dependent disease resistance. Science **301:** 969–972.

Norambuena, L., Marchant, L., Berninsone, P., Hirschberg, C.B., Silva, H., and Orellana, A. (2002). Transport of UDP-galactose in plants. Identification and functional characterization of AtUTr1, an *Arabidopsis thaliana* UDP-galactos/UDP-glucose transporter. J. Biol. Chem. **277:** 32923–32929.

Norambuena, L., Nilo, R., Handford, M., Reyes, F., Marchant, L., Meisel, L., and Orellana, A. (2005). AtUTr2 is an *Arabidopsis thaliana* nucleotide sugar transporter located in the Golgi apparatus capable of transporting UDP-galactose. Planta **222:** 521–529.

O'Neill, M.A., Eberhard, S., Albersheim, P., and Darvill, A.G. (2001). Requirement of borate cross-linking of cell wall rhamnogalacturonan II for *Arabidopsis* growth. Science **294:** 846–849.

Ordenes, V.R., Reyes, F.C., Wolff, D., and Orellana, A. (2002). A thapsigargin-sensitive $Ca^{(2+)}$ pump is present in the pea Golgi apparatus membrane. Plant Physiol. **129:** 1820–1828.

Pata, M.O., Hannun, Y.A., and Ng, C.K. (2010). Plant sphingolipids: Decoding the enigma of the Sphinx. New Phytol. **185:** 611–630.

Pauly, M., Andersen, L.N., Kauppinen, S., Kofod, L.V., York, W.S., Albersheim, P., and Darvill, A. (1999). A xyloglucan-specific endo-β-1,4-glucanase from *Aspergillus aculeatus*: Expression cloning in yeast, purification and characterization of the recombinant enzyme. Glycobiology **9:** 93–100.

Pavet, V., Olmos, E., Kiddle, G., Mowla, S., Kumar, S., Antoniw, J., Alvarez, M.E., and Foyer, C.H. (2005). Ascorbic acid deficiency activates cell death and disease resistance responses in *Arabidopsis*. Plant Physiol. **139:** 1291–1303.

Poster, J.B., and Dean, N. (1996). The yeast VRG4 gene is required for normal Golgi functions and defines a new family of related genes. J. Biol. Chem. **271:** 3837–3845.

Prime, T.A., Sherrier, D.J., Mahon, P., Packman, L.C., and Dupree, P. (2000). A proteomic analysis of organelles from *Arabidopsis thaliana*. Electrophoresis **21:** 3488–3499.

Reuhs, B.L., Glenn, J., Stephens, S.B., Kim, J.S., Christie, D.B., Glushka, J.G., Zablackis, E., Albersheim, P., Darvill, A.G., and O'Neill, M.A. (2004). l-Galactose replaces l-fucose in the pectic polysaccharide rhamnogalacturonan II synthesized by the l-fucose-deficient *mur1 Arabidopsis* mutant. Planta **219:** 147–157.

Reyes, F., León, G., Donoso, M., Brandizzí, F., Weber, A.P.M., and Orellana, A. (2010). The nucleotide sugar transporters AtUTr1 and AtUTr3 are required for the incorporation of UDP-glucose into the endoplasmic reticulum, are essential for pollen development and are needed for embryo sac progress in *Arabidopsis thaliana*. Plant J. **61:** 423–435.

Reyes, F., and Orellana, A. (2008). Golgi transporters: Opening the gate to cell wall polysaccharide biosynthesis. Curr. Opin. Plant Biol. **11:** 244–251.

Robert-Seilaniantz, A., Grant, M., and Jones, J.D.G. (2011). Hormone crosstalk in plant disease and defense: More than just jasmonate-salicylate antagonism. Annu. Rev. Phytopathol. **49:** 317–343.

Rollwitz, I., Santaella, M., Hille, D., Flügge, U.I., and Fischer, K. (2006). Characterization of AtNST-KT1, a novel UDP-galactose transporter from *Arabidopsis thaliana*. FEBS Lett. **580:** 4246–4251.

Seifert, G.J., Barber, C., Wells, B., Dolan, L., and Roberts, K. (2002). Galactose biosynthesis in *Arabidopsis*: Genetic evidence for substrate channeling from UDP-D-galactose into cell wall polymers. Curr. Biol. **12:** 1840–1845.

Seino, J., Ishii, K., Nakano, T., Ishida, N., Tsujimoto, M., Hashimoto, Y., and Takashima, S. (2010). Characterization of rice nucleotide sugar transporters capable of transporting UDP-galactose and UDP-glucose. J. Biochem. **148:** 35–46.

Smith, C.K., and Fry, S.C. (1999). Biosynthetic origin and longevity in vivo of α-d-mannopyranosyl-(1 —> 4)-α-d-glucuronopyranosyl-(1 —> 2)-myo-inositol, an unusual extracellular oligosaccharide produced by cultured rose cells. Planta **210:** 150–156.

Sperling, P., Franke, S., Lüthje, S., and Heinz, E. (2005). Are glucocerebrosides the predominant sphingolipids in plant plasma membranes? Plant Physiol. Biochem. **43:** 1031–1038.

Sperling, P., and Heinz, E. (2003). Plant sphingolipids: Structural diversity, biosynthesis, first genes and functions. Biochim. Biophys. Acta **1632:** 1–15.

Surplus, S.L., Jordan, B.R., Murphy, A.M., Carr, J.P., Thomas, B., and Mackerness, S.A.H. (1998). Ultraviolet-B-induced responses in *Arabidopsis thaliana*: Role of salicylic acid and reactive oxygen species in the regulation of transcripts encoding photosynthetic and acidic pathogenesis-related proteins. Plant Cell Environ. **21:** 685–694.

Ternes, P., Feussner, K., Werner, S., Lerche, J., Iven, T., Heilmann, I., Riezman, H., and Feussner, I. (2011). Disruption of the ceramide synthase LOH1 causes spontaneous cell death in *Arabidopsis thaliana*. New Phytol. **192:** 841–854.

Torres, M.A. (2010). ROS in biotic interactions. Physiol. Plant. **138:** 414–429.

Vlot, A.C., Dempsey, D.A., and Klessig, D.F. (2009). Salicylic acid, a multifaceted hormone to combat disease. Annu. Rev. Phytopathol. **47:** 177–206.

Wang, W., et al. (2008). An inositolphosphorylceramide synthase is involved in regulation of plant programmed cell death associated with defense in *Arabidopsis*. Plant Cell **20:** 3163–3179.

Weigel, D., and Glazebrook, J. (2002). *Arabidopsis*: A Laboratory Manual. (Cold Spring Harbor, NY: Cold Spring Harbor Laboratory Press).

Weymann, K., Hunt, M., Uknes, S., Neuenschwander, U., Lawton, K., Steiner, H.Y., and Ryals, J. (1995). Suppression and restoration of lesion formation in *Arabidopsis lsd* mutants. Plant Cell **7:** 2013–2022.

Wheeler, G.L., Jones, M.A., and Smirnoff, N. (1998). The biosynthetic pathway of vitamin C in higher plants. Nature **393:** 365–369.

Wildermuth, M.C., Dewdney, J., Wu, G., and Ausubel, F.M. (2001). Isochorismate synthase is required to synthesize salicylic acid for plant defence. Nature **414:** 562–565.

Worrall, D., Ng, C.K., and Hetherington, A.M. (2003). Sphingolipids, new players in plant signaling. Trends Plant Sci. **8:** 317–320.

Wulff, C., Norambuena, L., and Orellana, A. (2000). GDP-fucose uptake into the Golgi apparatus during xyloglucan biosynthesis requires the activity of a transporter-like protein other than the UDP-glucose transporter. Plant Physiol. **122:** 867–877.

Zablackis, E., York, W.S., Pauly, M., Hantus, S., Reiter, W.D., Chapple, C.C., Albersheim, P., and Darvill, A. (1996). Substitution of L-fucose by L-galactose in cell walls of *Arabidopsis mur1*. Science **272:** 1808–1810.

Zhang, B., Liu, X., Qian, Q., Liu, L., Dong, G., Xiong, G., Zeng, D., and Zhou, Y. (2011). Golgi nucleotide sugar transporter modulates cell wall biosynthesis and plant growth in rice. Proc. Natl. Acad. Sci. USA **108:** 5110–5115.